Polariton Condensation in Gap-Confined States of Photonic Crystal Waveguides

F. Riminucci,[1] A. Gianfrate,[2] D. Nigro,[3] V. Ardizzone,[2] S. Dhuey,[1] L. Francaviglia,[1] K. Baldwin,[4] L. N. Pfeiffer,[4] D. Ballarini,[2] D. Trypogeorgos,[2] A. Schwartzberg,[1] D. Gerace,[3] and D. Sanvitto[2,*]

[1]*Molecular Foundry, Lawrence Berkeley National Laboratory, One Cyclotron Road, Berkeley, California 94720, USA*
[2]*CNR Nanotec, Institute of Nanotechnology, via Monteroni, 73100 Lecce, Italy*
[3]*Dipartimento di Fisica, Università di Pavia, via Bassi 6, 27100, Pavia, Italy*
[4]*PRISM, Princeton Institute for the Science and Technology of Materials, Princeton University, Princeton, New Jersey 08540, USA*

(Received 22 May 2023; revised 27 September 2023; accepted 1 November 2023; published 13 December 2023)

The development of patterned multiquantum well heterostructures in GaAs/AlGaAs waveguides has recently made it possible to achieve exciton-polariton condensation in a topologically protected bound state in the continuum (BIC). Polariton condensation was shown to occur above a saddle point of the two-dimensional polariton dispersion in a one-dimensional photonic crystal waveguide. A rigorous analysis of the condensation phenomenon in these systems, as well as the role of the BIC, is still missing. In the present Letter, we theoretically and experimentally fill this gap by showing that polariton confinement resulting from the negative effective mass and the photonic energy gap in the dispersion play a key role in enhancing the relaxation toward the condensed state. In fact, our results show that low-threshold polariton condensation is achieved within the effective trap created by the exciting laser spot, regardless of whether the resulting confined mode is long-lived (polariton BIC) or short-lived (lossy mode). In both cases, the spatial quantization of the polariton condensate and the threshold differences associated to the corresponding state lifetime are measured and characterized. For a given negative mass, a slightly lower condensation threshold from the polariton BIC mode is found and associated to its reduced radiative losses, as compared to the lossy one.

DOI: 10.1103/PhysRevLett.131.246901

Introduction.—Exciton-polaritons are elementary excitations that arise from the strong radiation-matter coupling between a long-lived photonic mode and an excitonic resonance. Their effects are enhanced when the excitonic field is confined in low-dimensional nanostructures, such as semiconductor quantum wells (QWs) made of inorganic semiconductors. As hybrid radiation-matter bosoniclike excitations, they represent a powerful platform for either nonlinear optics applications [1–5], including electrically pumped polariton lasers [6] or studying fundamental physics phenomena such as out of thermal equilibrium Bose-Einstein condensation [7–9] and superfluidity [10,11]. To date, exciton-polariton condensation has been mostly limited to planar microcavities with large Q factors based on distributed Bragg reflector mirrors. A great effort has been devoted to laterally confine microcavity polaritons to engineer the potential landscape [8,12–14], which has previously allowed to achieve condensation from negative-mass states in patterned microcavities [15–17]. Recently, polariton condensation has also been achieved in one-dimensional photonic crystal waveguides, without bottom and top Bragg mirrors, by exploiting QW exciton coupling to a long-lived photonic bound state in the continuum (BIC) [18,19]. In these experiments, exciton-polaritons were shown to accumulate in the low energy BIC mode at normal incidence, just above a saddle point of the energy dispersion, and separated by an energy gap from a minimum-energy radiative state (lossy branch) [20–22]. Despite the lack of Bragg mirrors, which greatly reduces the complexity of the heterostructure, the design still guarantees a low condensation threshold previously attributed to suppression of radiative losses through symmetry protection of the eigenmodes [23]. However, a full theoretical and experimental account of the condensation mechanism, especially when considering the role of the negative effective mass around the saddlelike polariton dispersion observed in [18], is still missing at the time of this writing, as well as the actual relevance of the BIC lifetime. A better understanding can potentially allow the study of non-Hermitian nanophotonic interfaces [24], or even the realization of lower-threshold lasers [19,25]. In this Letter, we unravel the critical role played by the negative mass and the energy gap between BIC and lossy modes in reaching the condensation onset in the saddle point observed in [18]. We present both experimental evidence and the results of a driven-dissipative theoretical model [26]. In particular, we emphasize the role of the blue-shifted negative-mass dispersion underneath the pump spot, which creates defect modes within an effective attractive potential, facilitating relaxation toward the condensed state. With respect to previous works [18,19], we are now able to fully control the location of the BIC from a saddle dispersion point to a minimum energy state. This allows one to gain

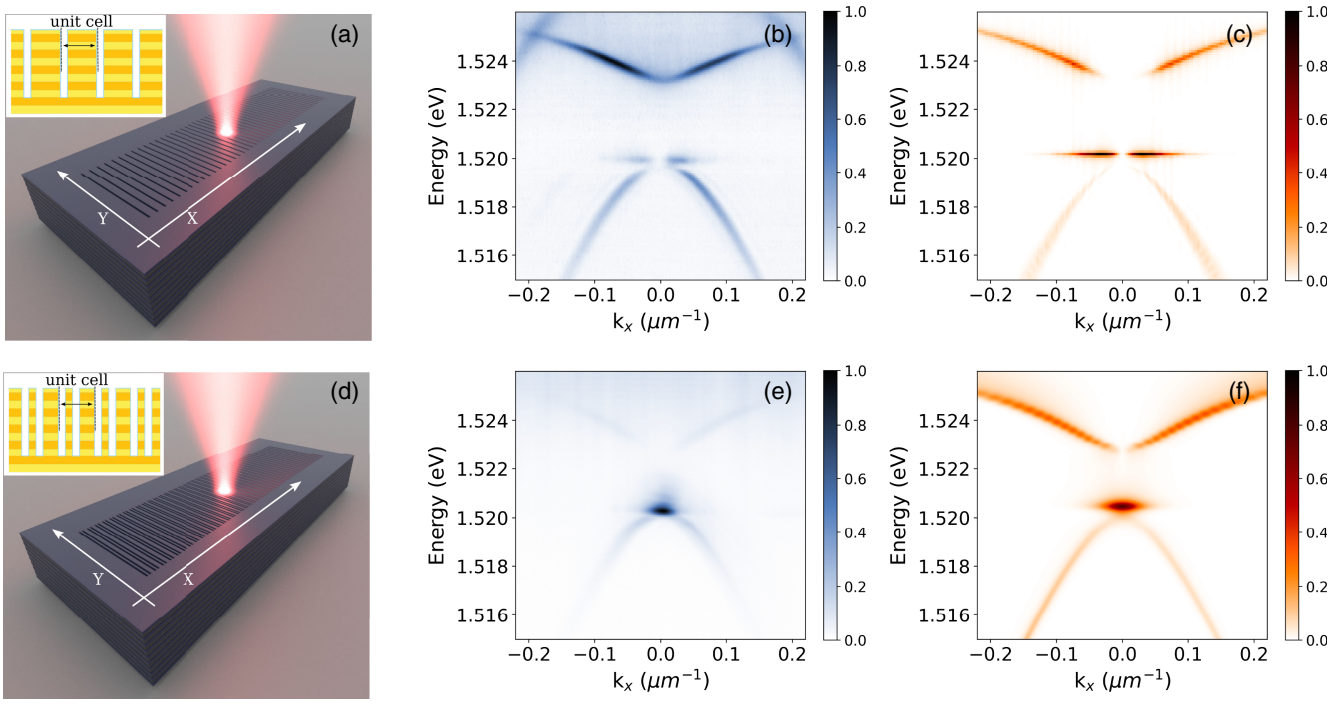

FIG. 1. Sketch of the etched subwavelength grating in the GaAs/AlGaAs heterostructures, and sample excitation and collection from the vertical direction supporting a dark (a) or bright (d) lower polariton branch. The insets show the cross section of the grating structure along the x direction in the two samples. Measured polariton dispersion along the photonic crystal waveguide supporting (b) a lower BIC and an upper lossy mode, and (e) a lower lossy and an upper BIC mode, respectively; gap-confined modes arising from either the BIC (b) or the lossy (e) branch, respectively, are clearly visible. The respective calculated excitonic fractions are 44% and 47% for these samples. (c),(f) Out-of-equilibrium GPE simulations of polariton emission for the two situations measured in (b) and (e), respectively.

insight into the importance of confinement during the thermalization process. Indeed, we achieve polariton condensation in gap-confined spatially quantized states, regardless of their BIC or lossy nature as induced by the symmetry properties of the lower-lying negative-mass branch. Finally, we also highlight the differences between the two cases, showing how the polariton radiative losses still play a role as demonstrated by the still lower threshold observed when condensation occurs in the gap-confined state arising from the negative-mass branch with a BIC at normal incidence.

Sample design and fabrication.—The fabricated sample is composed of a waveguide core made of 12 GaAs QWs 20 nm thick and 13 $Al_{0.4}Ga_{0.6}As$ barriers grown on an $Al_{0.8}Ga_{0.2}As$ cladding layer. On the same chip, we fabricated two different one-dimensional (1D) photonic crystal lattices etched in 170 nm deep grooves, which allowed us to engineer the polariton dispersion around normal incidence with the presence of either a BIC or a lossy photonic mode separated by an energy gap, as schematically shown in Figs. 1(a) and 1(d). Differently from previous works [18,19], here we etched deeper grooves in order to create a larger energy gap between upper and lower branches, whose BIC and lossy nature can be exchanged as a function of the air fraction [19,22]. The QWs in the waveguide core support exciton resonances that are strongly coupled to the photonic modes, giving rise to polariton branches whose symmetry properties are derived from the ones of the corresponding photonic coupled modes [27]. In fact, the details of the lattice geometry, such as air fraction or number of grooves in the unit cell, determine whether the maximum energy point in the dispersion is a BIC [as seen, e.g., in Figs. 1(b) and 1(c)] or a lossy mode [e.g., Figs. 1(e) and 1(f)]. Numerical simulations of the optical response from these structures performed with a Maxwell solver are given in Supplemental Material (SM) [28]. In particular, the photonic crystals designs were performed by using the Stanford Stratified Structure Solver (S4).[29].

Experiments.—Measurements are performed in a cryostat at 4 K, and uncoupled excitons and polaritons are introduced by nonresonant pumping onto the grating with a laser tuned at 1.59 eV, with a 12 μm FWHM spot. All measurements were taken using a single mode continuous wave laser. However for threshold characterization we used a pulsed laser with 80 MHz repetition rate and 100 fs pulse width to avoid spurious thermal effects that could arise at high pump powers under continuous wave excitation. As the excitons diffuse in each QW plane, we expect the potential well to spatially broaden. The photoluminescence (PL) signal (at around ∼1527.5 meV) is collected through a 3 cm focal length air spaced doublet and the real or

reciprocal space plane is reconstructed on the monochromator slits connected to a charged coupled device. At low excitation power, PL emission clearly evidences the dispersion of exciton-polariton branches, corresponding to extended modes along the 1D lattice. On the other hand, on increasing power, at the onset for polariton condensation, a dispersionless mode appears in the energy gap, hence gap-confined mode, arising from the negative-mass polariton band below the exciton line. The PL emission pattern in the energy-momentum space is shown to inherit features uniquely determined by the underlying photonic mode and the corresponding lattice geometry, with a dark [Fig. 1(b)] or bright [Fig. 1(e)] emission profile around $k_x = 0\ \mu\text{m}^{-1}$ [19,22,30], clear signature of the presence or absence of a photonic BIC, respectively. In fact, an unexpected outcome of this Letter, polariton condensation takes place in the gap-confined mode even if it arises from a lossy branch. This indicates that the mode topological properties and the associated radiative lifetime play a secondary role in the condensation phenomenon itself, suggesting a crucial contribution of the negative polariton mass despite only along one direction of the saddlelike dispersion in the lower branch.

Theoretical modeling.—In order to describe the condensation phenomenology shown from experiments, we resort to the formulation of an out-of-equilibrium Gross-Pitaevskii equation (GPE) under incoherent pumping [31], which allows us to include the effects of exciton-photon dispersion and exciton-photon coupling in describing the dynamics of the system. Here, we extend the previous formulation from Wouters and Carusotto [32], including the effects of multiband photonic dispersions coupled to the QW exciton modes, wave-vector-dependent loss rates within the single photonic band (distinguishing between BIC and lossy branches at $k = 0\ \mu\text{m}^{-1}$), and allowing for a confining potential created by the driven exciton population and described by a Gaussian function $P(x) = V_0 \exp\{-x^2/2\sigma^2\}$, where 2σ represents the spatial extent of the well, and V_0 its amplitude in meV. After solving for the multiband polariton wave function (polariton state vector), emission can be calculated from the photonic components of each polariton eigenmode, after superimposing the positive and negative group velocity modes from each branch. An example of such emission calculations is shown in Figs. 1(c) and 1(f), where the gap-confined modes appear with the right symmetry inherited from the corresponding negative-mass branch. Details of this extended formulation are summarized in SM, and a complete analysis of this model solutions has been recently reported [26]. We should notice that a 1D model is employed here, thus neglecting the full 2D dynamics induced, e.g., by the saddlelike dispersion of the lower branch, which does not seem crucial to correctly reproduce the experimental results.

Gap-confined modes and condensation threshold.—By increasing the laser power, we observed different quantized (i.e., dispersionless) modes arising underneath the pumping spot. This effect was observed for both the BIC and lossy polariton modes, respectively. In Fig. 2 we show the PL emission resolved in real space, in which we clearly see a fundamental mode (M0) and first excited (M1) mode, for polariton condensates arising from either the BIC [in Figs. 2(a) and 2(b)] or the lossy negative-mass branch [Figs. 2(c) and 2(d)]. The mode ordering is such that the M0 is higher in energy as compared to the M1, as it is appropriate for a negative-mass confinement. Since the photonic properties of BIC and lossy are naturally transferred to the corresponding polaritonic modes and condensate, the fundamental mode M0 will have an antisymmetric or a symmetric emission profile, respectively. For the sake of completeness, in the insets of Figs. 2(a) and 2(c) we report also the 2D emission profiles in real space at the same excitation power, which show their elongation along the lattice direction. The 1D spatially dependent profiles of these modes for all the considered cases were also extracted from the out-of-equilibrium GPE solution, when assuming a potential $V_0 = 1.25$ meV. These results are superimposed to the experimental plots in Figs. 2(b) and 2(d) (i.e., 1D cuts extracted from the full 2D experimental profiles), showing an excellent agreement. The interpretation is straightforward: a local blue shift of the polariton dispersion is induced by the pump spot, which creates confined polariton states within the energy gap; the latter, in turn, has a photonic origin due to the dielectric profile modulation introduced from the lattice. This local blue shift creates an effective Gaussian-like potential well in which negative-mass excitations are confined. For polaritons, scattering outside the blue-shifted area can occur at high momenta propagating modes that are resonant with the saddlelike dispersion outside the excitation region, while they are confined in a 20° conelike area along the periodicity direction as determined by the negative mass (see SM for details). Furthermore, the negative mass is responsible for the presence of a trapping potential for polaritons, thus enhancing the relaxation toward the condensed mode as well [12]. As long as the energy blue shift induced by the pump spot does not overcome the energy gap, the available states within the well are gap-confined [18].

To clarify the role of polariton lifetime on the condensation mechanism, we performed power series measurements that allowed us to observe the thresholds in the two cases considered in Fig. 1, in which the BIC or the lossy mode are alternatively coming from the negative-mass dispersion. The two cases have similar excitonic fraction associated with the energy state giving rise to the polariton condensate. Specifically, it is 44% for the BIC and 47% for the lossy mode, and their respective thresholds are shown in Fig. 3(a). The condensation in the lossy state [red dots in Fig. 3(a)] occurs at a higher power as compared to the one in the polariton BIC [blue dots in Fig. 3(a)]. The only meaningful difference between the two situations is related

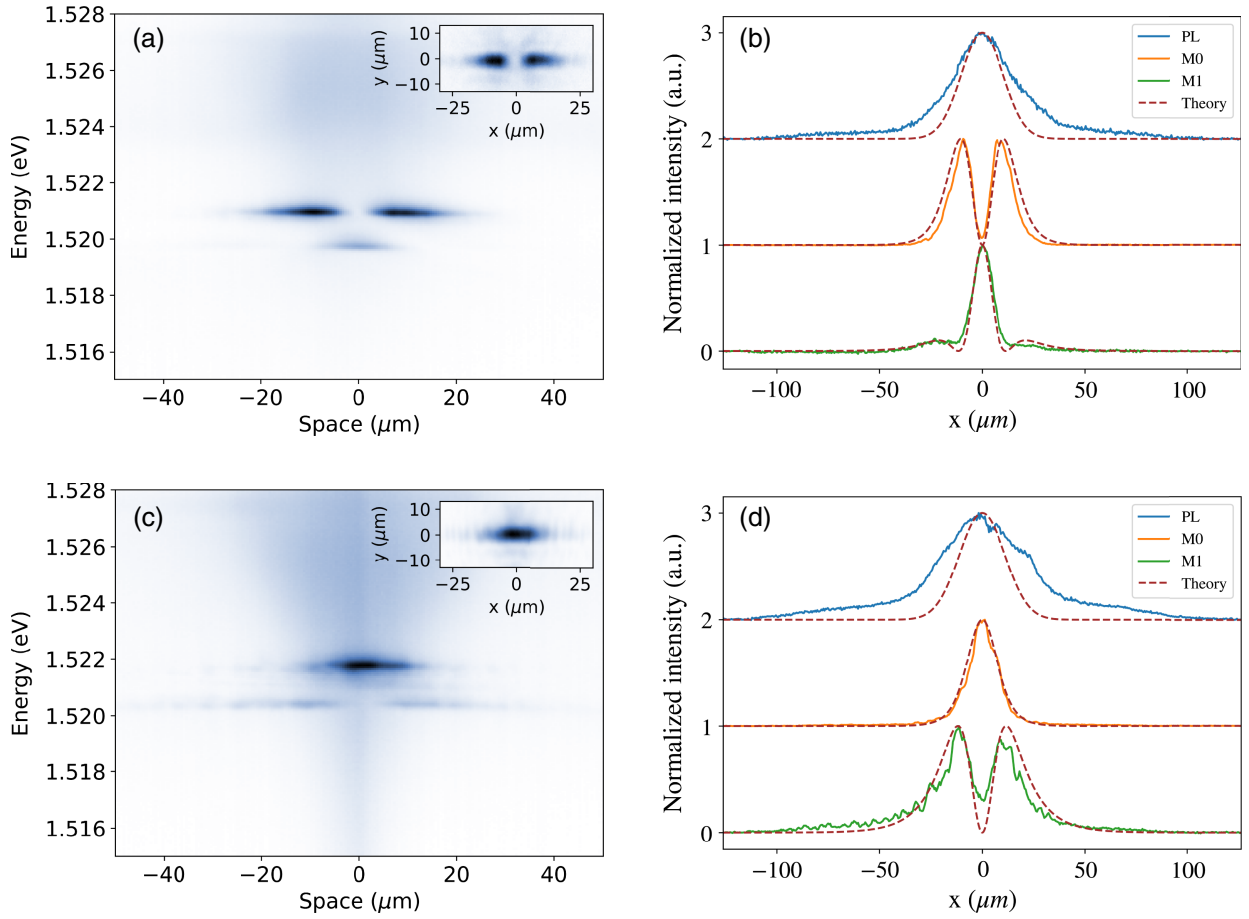

FIG. 2. Emission from quantized polariton condensate modes, with a fundamental (M0) and first excited (M1) state within the potential well created by the exciting laser spot, arising from either a BIC [(a),(b)] or a lossy [(c),(d)] lower branch. The insets also show the 2D spatial emission of the two M0 modes. In panels (b),(d) the x dependence of the measured luminescence is directly compared to the spatially resolved emission simulated through the 1D out-of-equilibrium GPE formulation (brown dashed lines). The measured exciton emission (blue line, corresponding to the broad and weak emission centered at 1527.5 meV) is compared to the Gaussian confining potential assumed in the simulations.

to the photonic losses of the relative condensed state. Below threshold, the slopes are the same for the two systems, indicating that both BIC and lossy modes are populated at the same rate through relaxation along the positive-mass branch of the lower polariton along k_y. However, the characteristic losses of each final state are different. As a matter of fact, a different slope above threshold is observed and shown in Fig. 3(a), with an estimated ratio of 1.97 ± 0.02 from the experimental data. As described in Ref. [32], the condensate density above threshold can be expressed as $|\Psi_0|^2 \propto 1/\gamma_c^{B,L}$, where $\gamma_c^{B,L}$ are the loss rates associated to the condensed mode that is either BIC (B) or Lossy (L). Although the BIC suppresses radiative losses, the condensate emits radiation in the far field at $k \neq 0$ μm^{-1}, as illustrated in Fig. 1(b). This results in a radiative contribution, denoted as γ_{rad}^B. The corresponding loss rate from the lossy state is identified as γ_{rad}^L, whereas all losses that do not arise from photon emission in the far field are included in γ_{nr}. Based on the rate equations described in SM, we can determine the ratio of power thresholds for the lossy and BIC, respectively, 410 W/cm^2 and 265 W/cm^2, to be

$$\frac{P_{\mathrm{th}}^L}{P_{\mathrm{th}}^B} = \frac{\gamma_{\mathrm{rad}}^L + \gamma_{\mathrm{nr}}}{\gamma_{\mathrm{rad}}^B + \gamma_{\mathrm{nr}}} = 1.55 \pm 0.04. \quad (1)$$

Even though the BIC is suppressing the radiative losses at exactly normal incidence, the condensate is still susceptible to radiative emission at finite angles and nonradiative recombination in the material. As a result, we attribute the lower threshold and steeper curve to the suppressed perpendicular emission from the polariton BIC. In contrast to the BIC, the lossy state has additional radiative losses causing a shorter lifetime, which increases the threshold and decreases the observed slope above threshold. Using a previously introduced model [27,33] and fitting the energy dispersions, we determine the linewidths $\gamma_{\mathrm{nr}} = 0.11$ meV and $\gamma_{\mathrm{rad}}^L + \gamma_{\mathrm{nr}} = 0.377$ meV (see SM). To rule out the

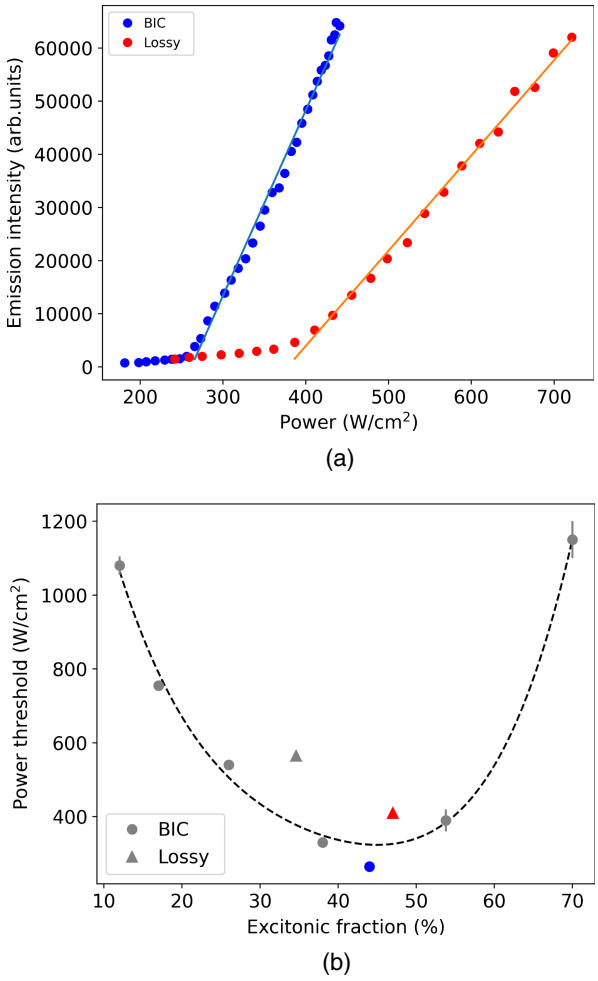

FIG. 3. (a) Condensate emission intensity from the BIC (blue dots) and the lossy gap-confined mode (red dots), respectively, plotted as a function of the incident laser power. (b) The gray circles and triangles represent the power thresholds measured on structures characterized by a condensate from a BIC and lossy, respectively, with different excitonic fractions. The fourth order polynomial fit through the condensation threshold from the BIC is represented by the dark dotted line. The condensate thresholds for the BIC and lossy shown in (a) are represented by the blue circle and red triangle, respectively.

possible role of the excitonic fraction, we show the condensation thresholds for different detunings in Fig. 3(b), when the condensation originates from a BIC (circles) or lossy (triangles) mode. The blue and red markers represent the thresholds measured in the samples under consideration in Fig. 3(a). The polynomial fit through the BIC condensation thresholds shows that the considered excitonic fractions should not play a relevant role. Therefore, we can make a meaningful comparison between the two photonic crystal designs. The optimal detuning that minimizes the condensation threshold is also found to be consistent with previous works [34,35]. This further confirms that the relaxation toward the condensed modes in our samples occurs through a positive-mass dispersion of the lower polariton branch along k_y. In fact, the effective mass along y is very similar to the one typically measured for conventional microcavity polaritons (see SM), and the same relaxation mechanisms are at play.

Summary.—We have shown the possibility to achieve polariton condensation driven by a negative-mass dispersion in a photonic crystal waveguide patterned on a multi-QW heterostructure, independently on whether the state in which the particles accumulate is a polariton BIC or a radiative polariton eigenmode. The spatial quantization is demonstrated by the discretization of the energy levels induced by a confining potential created by the pumping spot itself, for both BIC and lossy modes. All these results have been successfully modeled by an extension of the 1D out-of-equilibrium GPE, including the effects of multiband strong coupling, wave-vector-dependent losses, and effective confining potential in plane. Finally, we studied the impact of photonic losses, observing changes in both the critical density and the dependence of the condensate population on the injection rate. This gives us the ability to estimate the ratio of losses between the two cases. From this analysis we can assert that while the BIC shows a lower threshold between the two cases, its longer lifetime is not the main factor to drive the condensation. Instead, our results show how the negative mass can be used to induce a trapping potential and drive the polariton thermalization in both cases toward the lower branch, thus triggering the condensation onset.

We thank Paolo Cazzato for technical support. The authors acknowledge the project PRIN-2017 "Interacting Photons in Polariton Circuits INPhoPOL" funded by the Ministry of University and Scientific Research (MUR), Grant No. 2017P9FJBS_001. Work at the Molecular Foundry was supported by the Office of Science, Office of Basic Energy Sciences, of the U.S. Department of Energy under Contract No. DE-AC02-05CH11231. We acknowledge the project FISR—C. N. R. Tecnopolo di nanotecnologia e fotonica per la medicina di precisione —CUP B83B17000010001, and "Progetto Tecnopolo per la Medicina di precisione, Deliberazione della Giunta Regionale" Grant No. 2117. This research is partly funded by the Gordon and Betty Moore Foundations EPiQS Initiative, Grant No. GBMF9615 to L. N. Pfeiffer, and by the National Science Foundation MRSEC Grant No. DMR 1420541. We acknowledge support from the Project "Hardware implementation of a polariton neural network for neuromorphic computing," the Joint Bilateral Agreement CNR-RFBR (Russian Foundation for Basic Research), Triennial Program 2021–2023, the Italian Ministry of Scientific Research (MUR) through the FISR2020–COVID, project "Sensore elettro-ottico a guida d'onda basato sull'interazione luce-materia" (WaveSense), Contract No. FISR2020IP_04324.

*daniele.sanvitto@nanotec.cnr.it

[1] C. Sturm, D. Tanese, H. S. Nguyen, H. Flayac, E. Galopin, A. Lemaître, I. Sagnes, D. Solnyshkov, A. Amo, G. Malpuech, and J. Bloch, All-optical phase modulation in a cavity-polariton Mach–Zehnder interferometer, Nat. Commun. **5**, 3278 (2014).

[2] D. G. Suárez-Forero, F. Riminucci, V. Ardizzone, N. Karpowicz, E. Maggiolini, G. Macorini, G. Lerario, F. Todisco, M. De Giorgi, L. Dominici, D. Ballarini, G. Gigli, A. S. Lanotte, K. West, K. Baldwin, L. Pfeiffer, and D. Sanvitto, Enhancement of parametric effects in polariton waveguides induced by dipolar interactions, Phys. Rev. Lett. **126**, 137401 (2021).

[3] Anton V. Zasedatelev, Anton V. Baranikov, Denis Sannikov, Darius Urbonas, Fabio Scafirimuto, Vladislav Yu Shishkov, Evgeny S. Andrianov, Yurii E. Lozovik, Ullrich Scherf, Thilo Stöferle, Rainer F. Mahrt, and Pavlos G. Lagoudakis, Single-photon nonlinearity at room temperature, Nature (London) **597**, 493 (2021).

[4] Biswajit Datta, Mandeep Khatoniar, Prathmesh Deshmukh, Félix Thouin, Rezlind Bushati, Simone De Liberato, Stephane Kena Cohen, and Vinod M. Menon, Highly nonlinear dipolar exciton-polaritons in bilayer MoS_2, Nat. Commun. **13**, 6341 (2022).

[5] Daniele Sanvitto and Stéphane Kéna-Cohen, The road towards polaritonic devices, Nat. Mater. **15**, 1061 (2016).

[6] Christian Schneider, Arash Rahimi-Iman, Na Young Kim, Julian Fischer, Ivan G. Savenko, Matthias Amthor, Matthias Lermer, Adriana Wolf, Lukas Worschech, Vladimir D. Kulakovskii, Ivan A. Shelykh, Martin Kamp, Stephan Reitzenstein, Alfred Forchel, Yoshihisa Yamamoto, and Sven Höfling, An electrically pumped polariton laser, Nature (London) **497**, 348 (2013).

[7] J. Kasprzak, M. Richard, S. Kundermann, A. Baas, P. Jeambrun, J. M. J. Keeling, F. M. Marchetti, M. H. Szymánska, R. André, J. L. Staehli, V. Savona, P. B. Littlewood, B. Deveaud, and Le Si Dang, Bose-Einstein condensation of exciton polaritons, Nature (London) **443**, 409 (2006).

[8] Yongbao Sun, Patrick Wen, Yoseob Yoon, Gangqiang Liu, Mark Steger, Loren N, Pfeiffer, Ken West, David W. Snoke, and Keith A. Nelson, Bose-Einstein condensation of long-lifetime polaritons in thermal equilibrium, Phys. Rev. Lett. **118**, 016602 (2017).

[9] Davide Caputo, Dario Ballarini, Galbadrakh Dagvadorj, Carlos Sánchez Muñoz, Milena De Giorgi, Lorenzo Dominici, Kenneth West, Loren N. Pfeiffer, Giuseppe Gigli, Fabrice P. Laussy, Marzena H. Szymanska, and Daniele Sanvitto, Topological order and thermal equilibrium in polariton condensates, Nat. Mater. **17**, 145 (2018).

[10] Alberto Amo, Jérôme Lefrère, Simon Pigeon, Claire Adrados, Cristiano Ciuti, Iacopo Carusotto, Romuald Houdré, Elisabeth Giacobino, and Alberto Bramati, Superfluidity of polaritons in semiconductor microcavities, Nat. Phys. **5**, 805 (2009).

[11] Giovanni Lerario, Antonio Fieramosca, Fábio Barachati, Dario Ballarini, Konstantinos S. Daskalakis, Lorenzo Dominici, Milena De Giorgi, Stefan A. Maier, Giuseppe Gigli, Stéphane Kéna-Cohen, and Daniele Sanvitto, Room-temperature superfluidity in a polariton condensate, Nat. Phys. **13**, 837 (2017).

[12] Yoseob Yoon, Jude Deschamps, Mark Steger, Ken W. West, Loren N. Pfeiffer, David W. Snoke, and Keith A. Nelson, Enhanced thermalization of exciton-polaritons in optically generated potentials, arXiv:2209.13703.

[13] C. Schneider, K. Winkler, M. D. Fraser, M. Kamp, Y. Yamamoto, E. A. Ostrovskaya, and S. Höfling, Exciton-polariton trapping and potential landscape engineering, Rep. Prog. Phys. **80**, 016503 (2017).

[14] Lydie Ferrier, Esther Wertz, Robert Johne, Dmitry D. Solnyshkov, Pascale Senellart, Isabelle Sagnes, Aristide Lemaître, Guillaume Malpuech, and Jacqueline Bloch, Interactions in confined polariton condensates, Phys. Rev. Lett. **106**, 126401 (2011).

[15] F. Baboux, D. De Bernardis, V. Goblot, V. N. Gladilin, C. Gomez, E. Galopin, L. Le Gratiet, A. Lemaître, I. Sagnes, I. Carusotto, M. Wouters, A. Amo, and J. Bloch, Unstable and stable regimes of polariton condensation, Optica **5**, 1163 (2018).

[16] Marijana Milićević, Olivier Bleu, Dmitry D. Solnyshkov, Isabelle Sagnes, Aristide Lemaître, Luc Le Gratiet, Abdelmounaim Harouri, Jacqueline Bloch, Guillaume Malpuech, and Alberto Amo, Lasing in optically induced gap states in photonic graphene, SciPost Phys. **5**, 064 (2018).

[17] D. Tanese, H. Flayac, D. Solnyshkov, A. Amo, A. Lemaître, E. Galopin, R. Braive, P. Senellart, I. Sagnes, G. Malpuech, and J. Bloch, Polariton condensation in solitonic gap states in a one-dimensional periodic potential, Nat. Commun. **4**, 1749 (2013).

[18] V. Ardizzone, F. Riminucci, S. Zanotti, A. Gianfrate, M. Efthymiou-Tsironi, D. G. Suàrez-Forero, F. Todisco, M. De Giorgi, D. Trypogeorgos, G. Gigli, K. Baldwin, L. Pfeiffer, D. Ballarini, H. S. Nguyen, D. Gerace, and D. Sanvitto, Polariton Bose–Einstein condensate from a bound state in the continuum, Nature (London) **605**, 447 (2022).

[19] F. Riminucci, V. Ardizzone, L. Francaviglia, M. Lorenzon, C. Stavrakas, S. Dhuey, A. Schwartzberg, S. Zanotti, D. Gerace, K. Baldwin, L. N. Pfeiffer, G. Gigli, D. F. Ogletree, A. Weber-Bargioni, S. Cabrini, and D. Sanvitto, Nanostructured GaAs/(Al,Ga)As waveguide for low-density polariton condensation from a bound state in the continuum, Phys. Rev. Appl. **18**, 024039 (2022).

[20] Chia Wei Hsu, Bo Zhen, A. Douglas Stone, John D. Joannopoulos, and Marin Soljačić, Bound states in the continuum, Nat. Rev. Mater. **1**, 16048 (2016).

[21] Vasily Kravtsov, Ekaterina Khestanova, Fedor A. Benimetskiy, Tatiana Ivanova, Anton K. Samusev, Ivan S. Sinev, Dmitry Pidgayko, Alexey M. Mozharov, Ivan S. Mukhin, Maksim S. Lozhkin, Yuri V. Kapitonov, Andrey S. Brichkin, Vladimir D. Kulakovskii, Ivan A. Shelykh, Alexander I. Tartakovskii, Paul M. Walker, Maurice S. Skolnick, Dmitry N. Krizhanovskii, and Ivan V. Iorsh, Nonlinear polaritons in a monolayer semiconductor coupled to optical bound states in the continuum, Light Sci. Appl. **9**, 56 (2020).

[22] Leran Lu, Quynh Le-Van, Lydie Ferrier, Emmanuel Drouard, Christian Seassal, and Hai Son Nguyen, Engineering a light–matter strong coupling regime in

perovskite-based plasmonic metasurface: Quasi-bound state in the continuum and exceptional points, Photonics Res. **8**, A91 (2020).

[23] Bo Zhen, Chia Wei Hsu, Ling Lu, A. Douglas Stone, and Marin Soljačić, Topological nature of optical bound states in the continuum, Phys. Rev. Lett. **113**, 257401 (2014).

[24] Ki Young Lee, Kwang Wook Yoo, Youngsun Choi, Gunpyo Kim, Sangmo Cheon, Jae Woong Yoon, and Seok Ho Song, Topological guided-mode resonances at non-Hermitian nanophotonic interfaces, Nanophotonics **10**, 1853 (2021).

[25] Ashok Kodigala, Thomas Lepetit, Qing Gu, Babak Bahari, Yeshaiahu Fainman, and Boubacar Kanté, Lasing action from photonic bound states in continuum, Nature (London) **541**, 196 (2017).

[26] Davide Nigro and Dario Gerace, Theory of exciton-polariton condensation in gap-confined eigenmodes, Phys. Rev. B **108**, 085305 (2023).

[27] Nguyen Ha My Dang, Simone Zanotti, Emmanuel Drouard, Céline Chevalier, Gaëlle Trippé-Allard, Mohamed Amara, Emmanuelle Deleporte, Vincenzo Ardizzone, Daniele Sanvitto, Lucio Claudio Andreani, Christian Seassal, Dario Gerace, and Hai Son Nguyen, Realization of polaritonic topological charge at room temperature using polariton bound states in the continuum from perovskite metasurface, Adv. Opt. Mater. **10**, 2102386 (2022).

[28] See Supplemental Material at http://link.aps.org/supplemental/10.1103/PhysRevLett.131.246901 for additional details on design, the out of equilibrium GPE simulations, the rate equations model accounting for condensation threshold, and additional data concerning the dispersion along k_y.

[29] Victor Liu and Shanhui Fan, S 4: A free electromagnetic solver for layered periodic structures, Comput. Phys. Commun. **183**, 2233 (2012).

[30] E. Maggiolini, L. Polimeno, F. Todisco, A. Di Renzo, M. De Giorgi, V. Ardizzone, R. Mastria, A. Cannavale, M. Pugliese, V. Maiorano, G. Gigli, D. Gerace, D. Sanvitto, and D. Ballarini, Strongly enhanced light-matter coupling of a monolayer WS2 from a bound state in the continuum, Nat. Mater. **22** 964 (2023).

[31] Iacopo Carusotto and Cristiano Ciuti, Quantum fluids of light, Rev. Mod. Phys. **85**, 299 (2013).

[32] Michiel Wouters and Iacopo Carusotto, Excitations in a nonequilibrium Bose-Einstein condensate of exciton polaritons, Phys. Rev. Lett. **99**, 140402 (2007).

[33] Antonio Gianfrate, Helgi Sigurdsson, Vincenzo Ardizzone, Hai Chau Nguyen, Fabrizio Riminucci, Maria Efthymiou-Tsironi, Kirk W. Baldwin, Loren N. Pfeiffer, Dimitrios Trypogeorgos, Milena De Giorgi, Dario Ballarini, Hai Son Nguyen, and Daniele Sanvitto, Optically reconfigurable molecules of topological bound states in the continuum, arXiv:2301.08477.

[34] J. Kasprzak, D. D. Solnyshkov, R. André, Le Si Dang, and G. Malpuech, Formation of an exciton polariton condensate: Thermodynamic versus kinetic regimes, Phys. Rev. Lett. **101**, 146404 (2008).

[35] Esther Wertz, Lydie Ferrier, Dmitry D. Solnyshkov, Pascale Senellart, Daniele Bajoni, Audrey Miard, Aristide Lemaître, Guillaume Malpuech, and Jacqueline Bloch, Spontaneous formation of a polariton condensate in a planar GaAs microcavity, Appl. Phys. Lett. **95**, 051108 (2009).